Author(s): Hovi, J.-P. & Lahtinen, J. & Liu, Z. S. & Nieminen, Risto M.

Title: Monte Carlo study of CO hydrogenation on cobalt model catalysts

Year: 1995

Version: Final published version

Please cite the original version:

Hovi, J.-P. & Lahtinen, J. & Liu, Z. S. & Nieminen, Risto M. 1995. Monte Carlo study of CO hydrogenation on cobalt model catalysts. Journal of Chemical Physics. Volume 102, Issue 19. 7674-7682. DOI: 10.1063/1.469019.

Monte Carlo study of CO hydrogenation on cobalt model catalysts

J.-P. Hovi, J. Lahtinen, Z. S. Liu, and R. M. Nieminen

Citation: The Journal of Chemical Physics **102**, 7674 (1995); doi: 10.1063/1.469019
View online: http://dx.doi.org/10.1063/1.469019
View Table of Contents: http://scitation.aip.org/content/aip/journal/jcp/102/19?ver=pdfcov
Published by the AIP Publishing

Monte Carlo study of CO hydrogenation on cobalt model catalysts

J.-P. Hovi,[a] J. Lahtinen,[b] Z. S. Liu, and R. M. Nieminen
Laboratory of Physics, Helsinki University of Technology, 02150 Espoo, Finland

(Received 23 December 1994; accepted 7 February 1995)

Useful information on catalytic reactions can be achieved using Monte Carlo simulations combined with experimental data from model catalysts. We present a comprehensive analysis of the simulation studies of CO hydrogenation on a hexagonal surface using a discrete computer model for the irreversible reaction kinetics with no interactions between the surface species but their mutual reactions. The simulation results are compared to experimental data from a cobalt foil model catalyst at 101 kPa and 525 K. As a result, the following microscopic picture of the reaction on the catalyst surface is extracted: the rate-limiting reaction step is the termination of the carbon chains (α-hydrogenation), hydrogen atoms occupy different adsorption sites from other reactants, and the diffusion of hydrogen along the surface is fast. The model is also used to address the relevance of the ensemble effects for CO dissociation and the surface sensitivity of the CO hydrogenation reaction. Our simulation results imply that these aspects have little effect on the rates of hydrocarbon formation. © *1995 American Institute of Physics.*

I. INTRODUCTION

The conventional way of modeling the surface reactions use the kinetic reaction equations for the elementary reaction steps. The equations are based on the assumption that the reaction scheme can be described in terms of average surface coverages, and that all the reaction intermediates are in dynamical equilibrium with each other.[1] These equations describing the elementary reaction steps form a large set of coupled differential equations, which is then solved subject to the assumption of the dynamical equilibrium.

Recently, there has been considerable interest in the modelling of the surface reactions using Monte Carlo (MC) techniques. In this approach the individual atoms or molecules are assumed to follow a set of stochastic rules which describe the elementary reaction steps, including adsorption and diffusion. The method allows high flexibility because e.g. different surface structures or ensemble effects can be easily included into the stochastic rules. Promising results have already been achieved for the CO oxidation[2–5] and for NO–CO reaction.[6] Until recently, the interest in these models has mainly focused on their critical and kinetic behavior, but their connection to experiments has not been investigated in detail.

Here we give an extensive report of application of MC simulations to obtain microscopic information on the surface reactions. This is achieved by combining the simulation results with experimental data obtained from a well characterized small area model catalyst. In this work we have studied the CO hydrogenation on a cobaltlike (hexagonal) surface, but a similar approach could also be used for other heterogenous catalysis reactions.

The reaction model is described in detail in Sec. II. The model is discrete and irreversible, and all the interactions in the catalyst system have been described by phenomenological parameters, e.g. the reaction probabilities. The model is based on the carbide reaction mechanism[8] and molecular CO adsorption. We utilize the model to predict how the activity and the product distribution of the catalyst change when the partial pressures of the reactive gases, here CO and H_2, are changed. The main advantage of the model is that its behavior is determined by a relatively small set of simulation parameters, e.g. the choice of the rate-limiting reaction step and rate of hydrogen diffusion, which describe microscopic interactions on the catalyst surface.

The model predictions (see Sec. III) are compared to the experimental pressure dependencies[7] giving a reasonable picture of the microscopic interactions on the catalyst surface. The most important features of the resulting microscopic picture are the rate-limiting elementary reaction step is the termination of carbon chains (α-hydrogenation), and the diffusion of hydrogen and the growth of carbon chains are fast processes. Comparison to the experimental data reveals that pressure dependencies of the rates of hydrocarbon formation are similar to the experiment, except for systematic deviations of the rate of C_{2+} formation at low CO pressures. The most serious drawback of the simulations is that the computer model tends to give a much lower selectivity towards methane than the experiments.

Having identified the simulation parameters which correspond to the experimental situation, we use the model to address the nature of the ensemble effect for the CO dissociation, and the structure sensitivity of the CO hydrogenation reaction. In these simulations we find that the ensemble size, i.e. the number of the vacant adsorption sites the dissociation demands, has no effect on the selectivity or the activity of the catalyst reaction, until the CO dissociation involves so many adsorption sites that catalyst becomes gradually poisoned with CO. It is also observed that the reaction model is not sensitive to the surface structure, but the model gives similar pressure dependencies for the rates of hydrocarbon formation on hexagonal and square surfaces.

Finally the simulation results are summarized and conclusions are presented in Sec. IV.

[a]Present address: Raymond and Beverly Sackler Faculty of Exact Sciences, School of Physics and Astronomy, Tel Aviv University, Ramat Aviv 69978, Tel Aviv, Israel.
[b]Corresponding author.

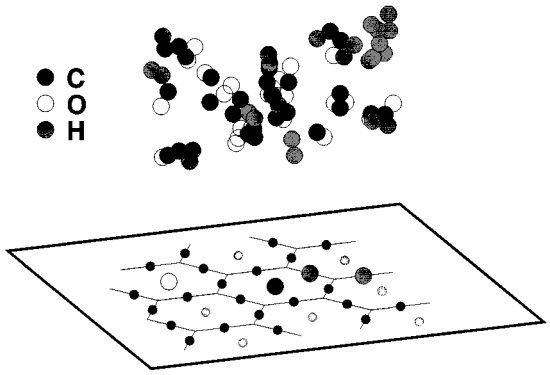

FIG. 1. The surface used in the model. The adsorption sites for CO (light small circles) form a hexagonal lattice, and between each CO site there is an adsorption site for hydrogen (dark small circles). Argon atoms, which are used as a fill-up gas to keep the total pressure constant, are not shown.

II. REACTION MODEL

Essential parts of the simulation algorithm are the catalyst surface, the reaction mixture, reactions with the surface (adsorption, desorption, and diffusion), and reactions between different adsorbants. We discuss these basic modules in more detail below.

A. Catalyst

The catalyst surface is modeled by a lattice with hexagonal symmetry. We have used different adsorption sites for C, O or their compounds (A sites), and hydrogen (B sites). The two-component lattice is illustrated in Fig. 1. The A sites form a triangular lattice, and there is one B site between each pair of A sites giving three times more B sites than A sites. The symmetry of the surface is that of the (0001) plane of any hcp metal, e.g. cobalt, or (111)-plane of any fcc metal. However, the identity of the adsorption sites (on-top, bridge) is left unspecified. The most essential feature is that CO and H_2 do not compete for the same adsorption sites. This assumption was found to be necessary in order to obtain a reactive steady state extending through a wide range of CO and H_2 partial pressures, while otherwise the catalyst becomes poisoned with CO or H atoms as in previous models for the CO oxidation.[2]

B. Reaction gas

The catalyst is embedded into a synthesis gas atmosphere. The partial pressures of CO and H_2 are p_{CO} and p_{H_2}, respectively. An inert gas component (like argon in the experiments) is used as a fill-up gas so that the total pressure of the mixture is constant (scaled to one) irrespective of the pressures of the reactants. The partial pressures are given in the beginning of the simulation and assumed to remain constant throughout the calculation. The partial pressure of a gas component, p, determines the number of molecules colliding with the surface per unit time through

$$Z_0 = \frac{p}{\sqrt{2\pi mkT}} = Ap/\sqrt{m}. \tag{1}$$

The constant A is the same for all gases, and we set $A \equiv 1$ which determines the connection between the real time and the simulation time. In order to simulate the net effect of competing sticking and (thermal) desorption, we have added an effective sticking coefficient S_{eff} into the model. Thus the collision frequency is given by $Z = S_{\text{eff}} p/\sqrt{m}$.

The reaction products are assumed to be separated from the reactants immediately after the desorption, and no readsorption can take place. These assumptions simulate well the reaction experiments in the limit of small conversion.

C. Adsorption

A molecule, CO, H_2, or Ar, is randomly chosen to hit the surface with the probability Z_{CO}, Z_H, or Z_{Ar}, respectively. According to the chosen molecule, different phenomena take place.

If the molecule is H_2, two neighboring B sites are chosen randomly. If both sites are vacant, the hydrogen molecule dissociates on the surface, and both adsorption sites are filled with a hydrogen atom. Otherwise the adsorption fails and the molecule bounces back to the gas phase.

If the molecule is CO, an A site is randomly chosen. If the site is vacant a CO molecule adsorbs on the surface

$$\text{CO} + * \rightarrow \text{CO}^*, \tag{2}$$

where $*$ denotes an empty adsorption site, and CO* stands for an adsorbed molecule. The CO molecule then dissociates with a given probability, provided that there is an empty nearest-neighbor A site

$$\text{CO}^* + * \rightarrow \text{C}^* + \text{O}^*, \tag{3}$$

but no CO desorption can take place.

D. Hydrogen diffusion

The diffusion of adsorbed species is an important part of the catalytic reaction. In this work we have considered hydrogen diffusion.

Let the hydrogen diffusion probability per unit time to be p_d. The diffusion step starts by taking a random number r from a binomial distribution with the expectation value $N_H p_d$, where N_H is the number of the hydrogen atoms on the surface. Then we repeat the following loop r times:

(1) Pick a random hydrogen atom on the surface.
(2) Check the nearest-neighbor hydrogen sites in a random order.
(3) If there is an empty site, move the atom to the vacant site.

In this way the same molecule can diffuse more than once during one unit of time.

E. Surface reactions

The elementary reactions considered in our model are based on the carbide mechanism.[8]

(1) The methane formation proceeds via stepwise hydrogenation of carbon,

$$\text{C}^* + \text{H}^* \rightarrow \text{CH}^* + *, \tag{4}$$

$$CH^*+H^* \rightarrow CH_2^*+*, \tag{5}$$

$$CH_2^*+H^* \rightarrow CH_3^*+*, \tag{6}$$

$$CH_3^*+H^* \rightarrow CH_4\uparrow+2*. \tag{7}$$

After the last reaction step the methane desorbs immediately from the surface.

(2) The hydrocarbon chains grow by addition of CH_2 groups to the alkyl species

$$C_nH_{2n+1}^*+CH_2^* \rightarrow C_{n+1}H_{2(n+1)+1}^*+*. \tag{8}$$

(3) The hydrocarbon chains terminate either by *α-hydrogenation*

$$C_nH_{2n+1}^*+H^* \rightarrow C_nH_{2n+2}\uparrow+2*, \tag{9}$$

producing alkanes or by *β-dehydrogenation*,

$$C_nH_{2n+1}^* \rightarrow C_nH_{2n}\uparrow+H^*, \tag{10}$$

producing alkenes. In the latter case the hydrogen atom remains on the A site until it reacts with an adsorbant on a neighboring A site, or diffuses to a neighboring B site.

(4) Water is formed from the adsorbed oxygen and hydrogen

$$O^*+H^* \rightarrow OH^*+*, \tag{11}$$

$$OH^*+H^* \rightarrow H_2O\uparrow+2*. \tag{12}$$

Each surface reaction has a specific reaction probability p_r (per unit time). Because the reaction model has no energy parameters (no temperature), the reaction probabilities give a simplified view of the actual catalytic process, and approximate the relative rates of different elementary reactions. It is also assumed that all these reaction intermediates are adsorbed on A sites, and therefore they block only the CO adsorption. The B sites are either vacant or filled with an adsorbed hydrogen. Furthermore, every reaction intermediate is adsorbed on a single adsorption site. In the case of the alkyl species this means that carbon chains are attached to the surface via one CH_2 radical, and grow away from the surface. These reaction steps were implemented by using a look-up table, and for practical reasons we have cut the chain growth after eight carbon atoms.

Reactions take place only between nearest-neighbor sites, and therefore the adsorbants on A and B sites behave differently on the surface. *Hydrogen* atoms can interact only with the two nearest A sites. Whenever a hydrogen atom is adsorbed or successfully diffused along the surface, it checks those two sites. *Adsorbates in the A sites* interact with their six nearest neighbor B sites, and also with the six nearest neighbor A sites. If an A site changes its state (after a CO adsorption or a reaction), first the B sites are checked in a random order and thereafter the A sites also in a random order.

We have been mostly interested in looking for the candidates for the rate limiting step of the synthesis. Then, for simplicity, most of the surface reactions are assumed to occur with a probability of one, except one or two rate limiting steps which are assumed to be drastically less probable than the other reactions. Typically, our candidates for the rate limiting reaction steps are either one of the CH_x+H reactions ($x=0,1,2$), or the α-hydrogenation.

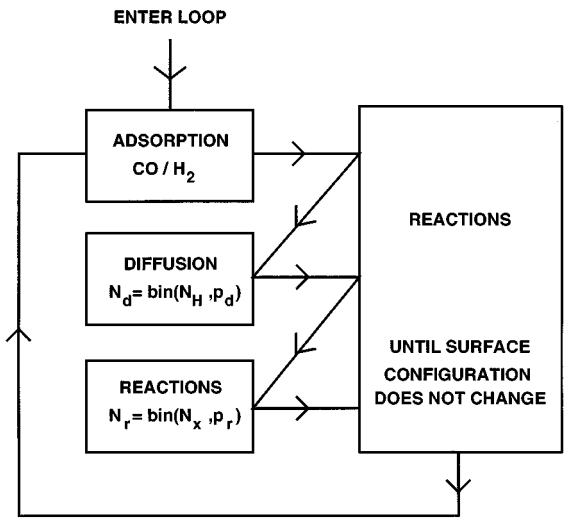

FIG. 2. The main loop of the simulation program. The number of atoms/molecules reacting or diffusing (N_r ,N_d) is calculated using the number of corresponding species on the surface (N_i) and the corresponding reaction probability per unit time (p_i).

Surface reactions are initiated by any change (e.g., adsorption, diffusion) in the state of the adsorption sites. This change can start an avalanche of the reactions. Because every surface reaction involves at least one A site, the changed sites are stored, and the reaction subroutine is called until no changes in the surface configuration occur. Therefore the reaction proceeds as a reaction front starting from the initial ''seed site,'' and terminates if there is no suitable reactive pair of adsorbants, or it stops at a low probability reaction step.

If the reaction terminates at a low probability reaction step, it will continue later with a probability p_r per unit time. After the adsorption and diffusion steps we draw a binomially distributed random number r with the expectation value of Np_r. Here N is the number of given reactants on the A site, because in order to save computer time, we keep track only of the number of adsorbates on the surface instead on the number of the pairs of adsorbants. We then pick randomly r reactants, for which the nearest-neighbor sites are checked and reacted with in random order. After this we continue to follow the reaction front further.

F. Simulation parameters

The main loop of the simulation program is given schematically in Fig. 2. One execution of the main loop defines the time unit of the model.

The parameters of the reaction model and their default values are summarized in Table I. For simplicity, we have ignored the β-dehydrogenation in most of the simulations, and in these cases all the reaction products are alkanes.

The partial pressure dependencies of the rate of hydrocarbon formation were determined by varying the partial pressure of one reactant while keeping the other constant,

TABLE I. Model parameters and their default values.

	Parameter	Default value
Reaction gas	CO partial pressure	0.25
	H partial pressure	0.55
Adsorption	CO effective sticking	1.0
	CO adsorption mechanism	molecular
	H_2 effective sticking	0.5
	H_2 adsorption mechanism	dissociative
Reactions	reaction probabilities,	1.0
	except β-dehydrogenation probability	0.0
Diffusion	hydrogen diffusion probability	0.0

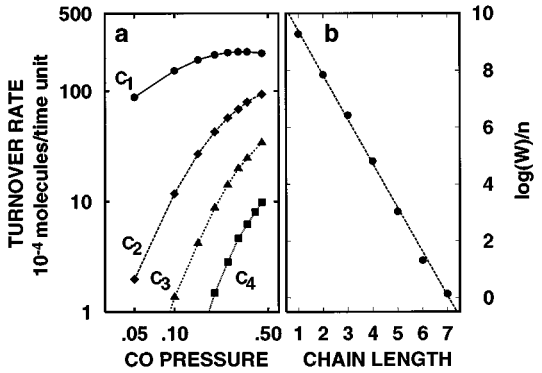

FIG. 3. (a) The rates of formation for C_{1-4} hydrocarbons as a function of CO partial pressure using the default values of the simulation parameters (shown in Table I). (b) Data for $p_{CO}=p_{H_2}=0.25$ plotted according to the AFS distribution. The dashed line is a least-squares fit of the AFS distribution to the simulated data yielding polymerization parameter $\alpha=0.212$.

and using ''argon'' as a fill-up gas. For CO pressure dependence simulations the H_2 pressure was held at 0.55, and for the H_2 pressure dependence the CO pressure was held at 0.25. These values correspond the pressures in the experimental measurements.[7]

We attempt to identify a suitable set of the reaction parameters for describing a real catalyst system. The connection between simulations and the experiments is provided by the partial pressures of CO and hydrogen.

All the simulations were started from an empty lattice. The lattice had 100×100 A sites with periodic boundary conditions. Performing a few test runs on larger systems we observed that the system size affects slightly the catalyst activity and the selectivity towards methane. For example, 150×150 system increases the activity approximately 10%. However, increasing the system size does not affect the pressure dependencies which are of the main interest in this work.

Typical simulation length was 6×10^6 time units. Given a set of the simulation parameters we monitored the product distribution and coverages on the catalyst surface. All the results in the next section are steady state values, given by averaging over the last 3×10^6 time units. Usually the averages are calculated from a single simulation only.

III. RESULTS AND DISCUSSION

We have used the reaction model to obtain information on the different microscopic aspects of CO hydrogenation on cobalt model catalysts. The simulation results are compared to the experimental data reported by Lahtinen *et al.*[7] Short accounts of different aspects of our early work are given in Refs. 11 and 12.

The most striking experimental feature of the Fischer–Tropsch synthesis is the negative CO partial pressure dependence of the methane production rate, which is observed on both supported[9] and on small area cobalt catalysts.[7] In the following section we show the results for the CO pressure dependence, because the hydrogen pressure dependence (especially that of the methane yield) was relatively well reproduced for quite a large set of parameter values.

A. Results using the default values of the parameters

The rate of formation of C_1–C_4 hydrocarbons as a function of the CO partial pressure is displayed in Fig. 3(a) using the default values for all the simulation parameters (see Table I). The rate of formation is defined as a number of hydrocarbons produced during one time unit per an A site.

The product distribution of simple polymerization can be described by the Anderson–Flory–Schultz (AFS) distribution

$$\log\left(\frac{W_n}{n}\right)=n\ \log\ \alpha+\log\left[\frac{(1-\alpha)^2}{\alpha}\right], \tag{13}$$

where W_n is the weight fraction of the hydrocarbons of length n, and α is the polymerization probability. The simulated data obeys well the AFS-distribution as depicted in Fig. 3(b) for $p_{CO}=p_{H_2}=0.25$. The polymerization probability of the AFS distribution calculated from data with the default parameter set is an increasing function of CO partial pressure, which varies from $\alpha=0.10$ ($p_{CO}=0.10$) to $\alpha=0.32$ ($p_{CO}=0.45$).

B. Searching for the rate-limiting reaction step

We have used the CH_x+H ($x=0,1,2$) reactions and the α-hydrogenation as candidates for the rate-limiting reaction step. The effect of each candidate is compared to the results of the previous subsection and to the experimental results.

1. Simulations excluding hydrogen diffusion

The turnover rates of the catalyst as a function of CO partial pressure using different rate-limiting step candidates are displayed in Fig. 4. The probability for the rate-limiting reaction step was set to 10^{-5}, giving approximately $2-6\times10^{-2}$ rate-limiting reactions during a time-unit (depending of the CH_x or alkyl coverage). The rest of the parameters had their default values.

If the rate-limiting step is C+H or CH+H [Figs. 4(a) and 4(b)] the catalyst yield mostly methane, and the rate of methane formation increases with increasing CO pressure. The methane yield also increases as a function of H_2 pressure (not shown here). Typically there is a large hydrogen coverage on the surface, and after passing the rate-limiting reaction step the CH or CH_2 molecule hydrogenates quickly, resulting in large methane yield and low chain growth. Highest

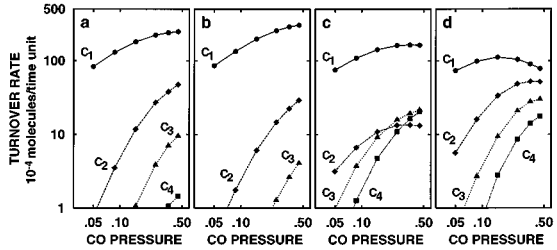

FIG. 4. Turnover rates for C_{1-4} hydrocarbons as a function of CO partial pressure using four different candidates for the rate limiting reaction step (a) C+H; (b) CH+H; (c) CH_2+H; and (d) α-hydrogenation. The probability of the rate limiting step is 10^{-5}. The rest of the simulation parameters had their default values.

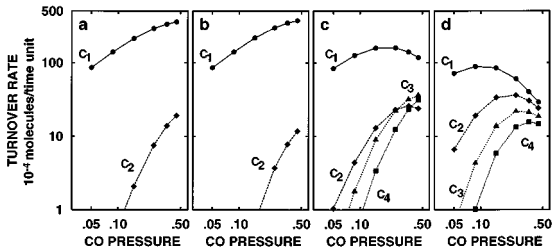

FIG. 5. Turnover rates for C_{1-4} with strongly diffusive hydrogen using four different candidates for the rate limiting reaction step (a) C+H; (b) CH+H; (c) CH_2+H; and (d) α-hydrogenation. The probability of the rate limiting step is 10^{-5}. The rest of the simulation parameters had their default values, except the hydrogen diffusion probability which was 10^{-3}.

selectivity towards methane is achieved when the rate-limiting step is CH+H. The production rate of methane increases as a function of CO partial pressure, because the CO consumption is only restricted by its availability.

If the rate-limiting step is CH_2+H [Fig. 4(c)], also detectable amounts of C_{2+} hydrocarbons are formed. The CH_2 coverage is very large, because the rate-limiting step blocks further hydrogenation, but the chain growth is limited by the small alkyl coverage. Most of the methyl molecules formed in the CH_2+H reaction hydrogenate to methane due to the large hydrogen coverage. However, if the methyl molecule does not hydrogenate, large CH_2 coverage can make the resulting carbon chain relatively long. This is the reason why the yield of C_{3-5} hydrocarbons can be larger than the ethane yield. The product distribution is thus modified in two ways. The methane yield is enhanced, and also the yield of long C_{3-5} hydrocarbons is larger than the ethane yield. The rate of methane formation still increases with increasing CO pressure.

If the rate-limiting step is α-hydrogenation [Fig. 4(d)], the yield of C_{2+} hydrocarbons is enhanced compared to the previous cases. The alkyl coverages are large because chain termination is slow. The alkyl and CH_2 coverages increase further, and the hydrogen coverage decreases with increasing CO pressure. In other words, the probability for chain growth increases and the probability for chain termination decreases with increasing CO partial pressure, resulting in a growing yield C_{2+} hydrocarbons. The polymerization probability of the AFS distribution is large, because the termination of the hydrocarbon chains becomes slow. The AFS polymerization parameter is an increasing function of the CO partial pressure, and reaches the value of 0.59 when p_{CO} is 0.45. However, the simulated trends of hydrocarbon formation rates are not in agreement with the experimental data.[7]

The simulations described above were carried out using a chain growth probability of one, but decreasing the chain growth probability below one does not drastically change the results. The natural consequence was a higher selectivity towards methane. We conclude that the reaction model does not reproduce the experimental trends without hydrogen diffusion.

Let us mention briefly that we were able to reproduce the negative CO partial pressure dependence in the rate of methane formation, if we added the possibility to terminate the chain growth by CH_3+alkyl reaction. However, this also modified the product distribution so that the rate of C_{2-4} formation was higher than that of methane. Based on the comparisons with the experimental product distribution[7] we considered this reaction path unrealistic.

2. Simulations including strongly diffusive hydrogen

As the next step we included the hydrogen diffusion and set the hydrogen diffusion probability to 10^{-3}. This means that on the average 5–20 hydrogen atoms diffuse during a time unit, i.e. the diffusion is much more frequent than all the adsorption or reaction processes. The rate of hydrocarbon formation as a function of CO partial pressure and for the different rate-limiting step candidates are displayed in Fig. 5.

If the rate-limiting step is CH_x+H, x=0,1,2 [Figs. 5(a)–5(c)], the rate of CO conversion is higher than without hydrogen diffusion. The effect grows as the CO partial pressure increases. However, the qualitative behavior of the catalyst is similar to that without diffusion.

If the rate-limiting step is α-hydrogenation [Fig. 5(d)], the rate of CO conversion is also enhanced up to 20% compared to the result without diffusion. In this case the experimental trend for the rate of methane formation is correctly reproduced. However, the rate of the chain growth is 2–3 times higher than without diffusion, and the AFS polymerization parameter varies from 0.10 to 0.77 as the CO partial pressures is increased from 0.05 to 0.45, giving a much larger α than in the experiments.

Comparing Figs. 4 and 5 we see that the hydrogen diffusion enhances the effect of the rate-limiting reaction step. In other words, diffusion favors fast surface reactions because every diffusing hydrogen attempts to react with the adsorbates on its new neighboring A sites. If the rate-limiting step is too slow, the hydrogen can diffuse away and react elsewhere.

From the data of Fig. 5(d) we calculated the turnover number of the CO molecules as a function of the CO partial pressure. The number of converted CO molecules is an increasing function of the partial pressure, which, however, contradicts the behavior of the experimental data. Throughout the calculated pressure range the ratio of successful CO adsorptions to the total number of CO adsorption trials remains large. As the CO pressure is increased from 0.05 to 0.45, the CO sticking is slowly decreased from 0.92 to 0.74,

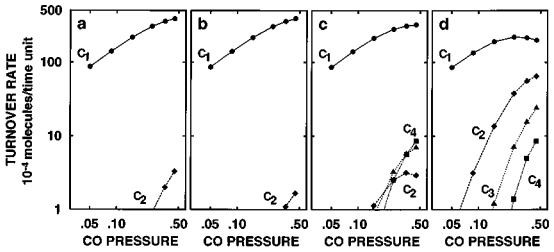

FIG. 6. Turnover rates for C_{1-4} with the chain growth probability of 10^{-4} using four different candidates for the rate limiting reaction step (a) C+H; (b) CH+H; (c) CH_2+H; and (d) α-hydrogenation. Other simulation parameters were as in Fig. 5.

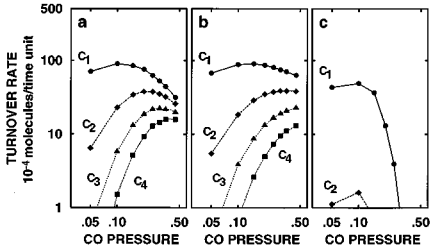

FIG. 7. Turnover rates for C_{1-4} with three different CO dissociation probabilities (a) 10^{-4}; (b) 10^{-5}; (c) 10^{-6}. The probabilities for the α-hydrogenation and hydrogen diffusion were 10^{-5} and 10^{-3}, respectively. Other simulation parameters had their default values.

if the initial sticking coefficient is one. Also the coverage of the CO molecules remains zero throughout the simulated pressure range due to the fast CO dissociation. These features tell that the model displays the negative pressure dependence of the methane formation because the catalyst selectivity is directed gradually towards the production of the C_{2+} hydrocarbon chains.

We repeated the calculations of this section setting the probability for the chain growth [Eq. (8)] to 10^{-4}. These results are shown in Fig. 6. We see that the decrease in the chain growth probability enhances the rate of methane formation and the number of produced C_{2+} hydrocarbons decreases. It is observed that at low chain growth probability the CO conversion rate is practically independent on the hydrogen diffusion probability. Especially, in case of the α-hydrogenation the observed negative CO pressure dependence of the methane yield disappears.

C. Slow CO dissociation or water formation

In this section we study the effects of the CO dissociation and OH+H reaction probabilities on the rates of hydrocarbon formation. The CO dissociation on cobalt surfaces is known to be slower than on iron surfaces,[13] and thus it is reasonable to test what effect the restricted dissociation has on the pressure dependence. On the other hand, the reduction of CoO has been proposed[14] to play an important role in CO and CO_2 hydrogenation. In these simulations this elementary reaction step would be represented by the O+H→OH reaction. However, in this section we show only the results for the restricted OH+H reaction, because the results for this reactions are very similar to those of the O+H reaction.

We varied the CO dissociation and OH+H reaction probabilities separately between 10^{-4} and 10^{-6}, using probabilities of 10^{-5} for α-hydrogenation and of 10^{-3} for the hydrogen diffusion and keeping the rest of the simulation parameters at their default values. The low α-hydrogenation probability was chosen because the results using the CO dissociation (or OH+H) probability of 10^{-5} together with the α-hydrogenation probability of 1.0 show *increasing* methane formation rate as a function of the CO partial pressure, excluding the possibility of these reactions being the true rate-limiting step.

The results with the CO dissociation probability p_d ranging from 10^{-4} to 10^{-6} are displayed in Fig. 7. We see that the rates of the hydrocarbon formation are not changed if $p_d=10^{-4}$ [Fig. 7(a)] but a decrease in the dissociation probability yields to larger selectivity towards methane and to the disappearance of the negative CO pressure dependence [Fig. 7(b)]. Finally, after a certain threshold the surface becomes saturated with CO molecules resulting in a drastic drop in the activity of the catalyst [Fig. 7(c)].

The changes observed with restricted water removal reaction are displayed in Fig. 8. The effect of this elementary reaction step are similar to those observed with restricted CO dissociation probability, except for the OH+H reaction probability 10^{-6} the rates of the hydrocarbon are only weakly pressure dependent instead of the catalyst poisoning. Especially, the decreased OH+H reaction probability leads to larger selectivity towards methane.

In both of these cases the lowered reaction probability yields to increased selectivity towards methane. The use of the reduced reaction probability generally leads to 20%–60% coverage of CO (OH) molecules and alkyls depending on the CO partial pressure, the rest of the surface being empty. The increased selectivity towards methane can be therefore directly attributed to the blocking of the chain growth by the CO (or OH) molecules.

Based on the simulations displayed in Figs. 7 and 8 we conclude that lowering these reaction probabilities result in the disappearance of the negative pressure dependence of the rate of the methane formation, and thus are not the rate limiting steps for the hydrogenation reaction.

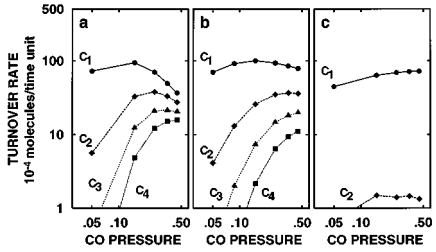

FIG. 8. Turnover rates for C_{1-4} with three different OH+H reaction probabilities (a) 10^{-4}; (b) 10^{-5}; (c) 10^{-6}. The probabilities for the α-hydrogenation and hydrogen diffusion were 10^{-5} and 10^{-3}, respectively. Other simulation parameters had their default values.

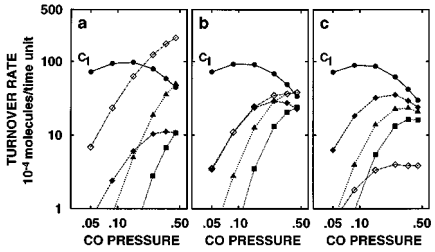

FIG. 9. Turnover rates C_{1-4} with three different β-dehydrogenation probabilities (a) 10^{-4}; (b) 10^{-5}; (c) 10^{-6}. Only the rates for ethane (solid diamonds) and ethene (open diamonds) are drawn separately, otherwise the rates for alkanes and alkenes are summed together. The probabilities for the α-hydrogenation and hydrogen diffusion were 10^{-5} and 10^{-3}, respectively. Other simulation parameters had their default values.

D. Including the β-dehydrogenation

So far all the simulations have ignored the β-dehydrogenation processes, and all the conclusions are based on the pressure dependence of the rate of methane formation. However, in the experiments most of the C_{2+} products are alkenes which implies that the β-dehydrogenation processes play a crucial role in the CO hydrogenation.

Therefore we repeated some of the calculations using the parameters which reproduce the experimental pressure dependence of the methane formation, and varied the β-dehydrogenation probability while keeping the rest of the simulation parameters at their default values. The simulation results for the β-dehydrogenation probabilities from 10^{-4} to 10^{-6} are displayed in Fig. 9.

We see that increasing the β-dehydrogenation probability from zero increases especially the ethane and ethene yield, because the β-dehydrogenation processes provide a fast route to chain termination in addition to the α-hydrogenation. Thus, due to this new channel for hydrocarbon formation, the product distribution follows the AFS distribution only for C_{2+} hydrocarbons.

If the β-dehydrogenation probability is larger than that of the α-hydrogenation, the catalyst yields more C_2 products than methane (Fig. 9). Although the product distribution in supported catalysts can exhibit low selectivity towards methane, the experimental product distribution in the cobalt foil model catalysts imply that the probability for β-dehydrogenation is smaller than the α-hydrogenation probability.

E. Comparison to the experimental results

Trying to keep the number of adjusted parameters as small as possible, we got a reasonable similarity between the simulation results and the experimental data when the probabilities for β-dehydrogenation, α-hydrogenation, chain growth, and hydrogen diffusion were set to 10^{-6}, 10^{-5}, 10^{-4}, and 10^{-3}, respectively and the effective sticking coefficient of hydrogen to 0.08. The simulation results using these parameters are compared to the experimental data in Fig. 10.

The simulation results in Fig. 10 show similar partial pressure dependencies as the experimental data, especially for methane. Furthermore, the calculated fraction of ethene in the C_2 products as a function of the partial pressure shows satisfactory similarity to the experimental data, and indicates

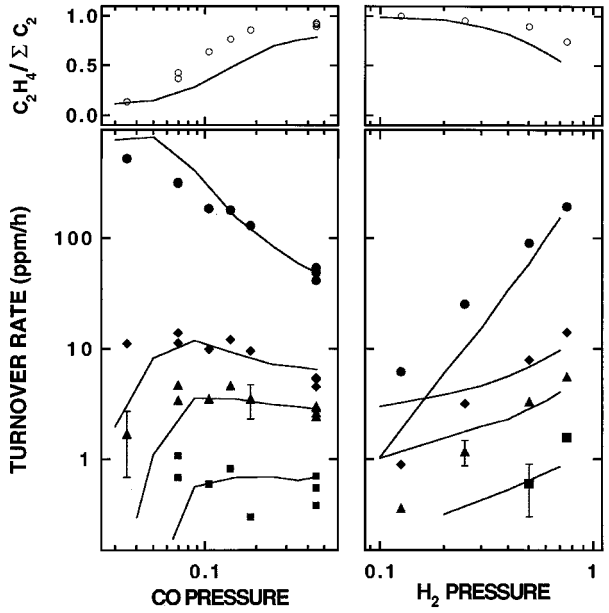

FIG. 10. Comparison of the partial pressure dependencies between the simulated hydrocarbon formation and the experimental data (at 525 K and 101 kPa) from Ref. 7. The fraction of ethene in the C_2 products (top) and the turnover rates of C_{1-4} hydrocarbons (main chart) are shown as a function of CO and H_2 partial pressure. The simulated data are shown by solid lines and the markers represent experimental data points; (○), ethene fraction; (●), C_1; (◆), C_2; (▲), C_3; and (■), C_4. The simulated data was multiplied by factors ν, 0.058ν, 0.035ν, and 0.012ν in case of C_1, C_2, C_3, and C_4, respectively, where ν connects the simulation time unit and the real time. As simulation parameters we used 10^{-6} for β-dehydrogenation, 10^{-5} for α-hydrogenation, 10^{-4} for chain growth, and 10^{-3} for hydrogen diffusion. Other reaction probabilities were set to one. The effective sticking coefficients were 0.08 and 1.0 for H_2 and CO, respectively.

that quite a large range of values can be reproduced. On the other hand, however, the selectivity towards methane is lower in the simulations than in the experiments, the results for the hydrogen pressure dependence for C_{2+} hydrocarbons are somewhat disappointing, and the CO pressure dependencies show systematic deviations at lowest CO pressures.

Of course, the results displayed in Fig. 10 represent a subjective compromise between different aspects of the experimental data. For example, better partial pressure dependencies can be achieved at the expense of ignoring the β-dehydrogenation processes, when all the reaction product are alkanes (see Fig. 3 in Ref. 11). Thus, better agreement with the experimental results clearly needs a more realistic model, including e.g. the real desorption processes and the allowing the elementary reactions to proceed in both directions. Especially, the hydrogen effective sticking coefficient gives only an estimate for the ratio of the sticking and desorption of H_2 relative to CO, and it is an assumption which neglects the competition between the desorption and the different elementary reactions. These amendments to the model are currently in progress.

As a first step towards the real desorption processes, we have performed a few test runs to study the effect of this simplification using sticking coefficients of one for both reactants and varying the rate of hydrogen desorption. The inclusion of slow hydrogen desorption gave similar cover-

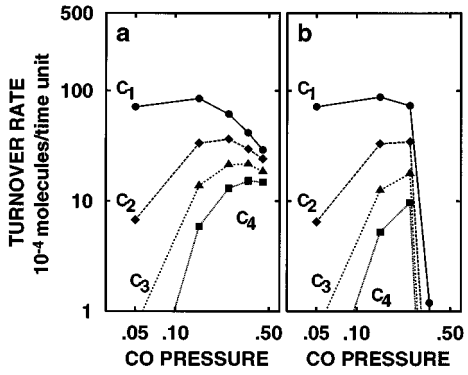

FIG. 11. Turnover rates for C_{1-4} with two different schemes modeling the ensemble effect; (a) three (b) four vacant A sites are required for the CO dissociation. The probabilities for the α-hydrogenation and hydrogen diffusion were 10^{-5} and 10^{-3}, respectively. Other simulation parameters had their default values.

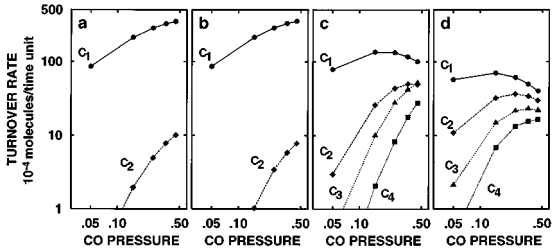

FIG. 12. Turnover rates for C_{1-4} on a square lattice using four different candidates for the rate limiting reaction step (a) C+H; (b) CH+H; (c) CH_2+H, and (d) α-hydrogenation. The probability of the rate limiting step is 10^{-5}. The rest of the simulation parameters had their default values, except the hydrogen diffusion probability which was set to 10^{-3}.

ages and rates of hydrocarbon formation than the use of an effective sticking coefficient of 0.3⋯0.5. In the limit of fast hydrogen desorption, the rates of hydrocarbon formation tend to become constants because the reaction rate is limited by the low hydrogen coverage.

F. Ensemble effects for the CO dissociation

It has been proposed that on a real catalyst surface reactions can require several adsorption sites.[16] For example, the adsorption of CO at low coverages takes place on the on-top sites[15] of the Co(0001) and Co(1010) surfaces. However, one can easily argue that the dissociation of CO will not take place at the on-top site, but a more highly coordinated adsorption site would be needed.[16] At higher coverages the presence of threefold coordinated CO molecules[15] and tilted or horizontal CO molecules[16] have been reported. We tested the effect of the ensemble size on the reactivity by requiring the presence of more than two adjacent vacant adsorption sites prior to the CO dissociation.

In the original model (here case 0) the dissociation takes place if a CO molecule has a vacant nearest neighbor A site, i.e. the dissociation involves pairs of A sites. The A sites form a triangular lattice, and therefore the sites in the pair have two nearest-neighbors in common. We studied the ensemble effects giving an additional requirement that the CO dissociation requires either one (case I) or both (case II) of common nearest-neighbors to be vacant. We used the simulation parameters which were found to correspond closely the experimental situation; the α-hydrogenation probability was set to 10^{-5}, and the hydrogen diffusion probability to 10^{-3} keeping the rest of the simulation parameters in their default value.

The simulation results are displayed in Fig. 11. For the case I, where the dissociation involves three adsorption sites, the rates of the hydrocarbon formation are the same as for the original model with the same simulation parameters within the statistical noise of 1%. The AFS polymerization parameter remains unchanged, and comparing the surface coverages in the original model and case I, we also find them identical. For case II, where the dissociation involves four adsorption sites, similar rates of the hydrocarbon formation, AFS polymerization parameter, and coverages are observed for $p_{CO}<0.20$, but at higher CO partial pressures the surface becomes eventually poisoned with CO.

Excluding the extreme case of the catalyst poisoning, we thus observe no ensemble effects for the activity of the catalyst, nor the polymerization parameter of the AFS distribution or the coverages are influenced. As a check we recalculated the simulation results for the case I using default set of the parameters, but observed no effects for that case either. This phenomenon is probably related to the fact that the reaction model operates in the reaction-controlled rather than adsorption-controlled limit.

G. Structure sensitivity

CO hydrogenation is reported to be structure insensitive on Ni, Ru,[17] and Mo (Ref. 18) surfaces and similar claims has been made concerning Rh and Fe surfaces.[19] On cobalt, the rate of methane formation is structure insensitive but enhancement in the production of higher molecular weight hydrocarbons has been seen on higher Miller-index surfaces.[10,20]

In order to address the question of the structure sensitivity, we have repeated some simulations on a surface where A sites form a square lattice, and there is one B site between each pair of A site giving two times more B sites than A sites. The symmetry of the lattice then corresponds to (100)-plane for any metal with a cubic primitive cell. In the context of the cobalt crystal we use the square lattice as a model to gain insight of CO hydrogenation on less densely packed (in terms of the nearest-neighbor adsorption sites) high-index surfaces, e.g. twofold coordinated (1120)-surface.[10]

Figure 12 shows the the rates of formation of C_{1-4} hydrocarbons using CH_x+H (x=0,1,2) reactions and the α-hydrogenation as candidates for the rate-limiting reaction step. The probability of the rate limiting step is 10^{-5} and the rest of the simulation parameters had their default values, except the hydrogen diffusion probability which was set to 10^{-3}. These results can be compared to the Fig. 5, which shows the simulation results for the same parameters and on the hexagonal surface. Comparing these figures we see that the structure sensitivity has little effect on the model behav-

ior. The figures show notable difference only in the case of the α-hydrogenation, when the square lattice has a slightly lower activity and the negative pressure dependence of the methanation rate is diminished as compared to the hexagonal surface. However, even in this case the trends in the rates of the hydrocarbon formation are very similar on the two surfaces.

From these simulations we conclude that the reaction model for the CO hydrogenation is not sensitive to the surface structure.

IV. CONCLUSIONS

We have studied the CO hydrogenation on a cobalt catalyst by irreversible and discrete computer model. The reaction model is based on the carbide reaction mechanism[8] and molecular CO adsorption. In this paper we show that the main features of CO hydrogenation can be modeled with a simple irreversible model giving useful information on certain microscopic details. These details include e.g. the rate-limiting reaction step and the effect of surface diffusion.

The simulations using various parameters yield different product distributions which can be compared to the experimental data. Concerning the rate-limiting step candidates and the rate of the hydrogen diffusion, our conclusions of the microscopic details are based solely on the negative pressure dependence of the methane formation rate, i.e. the sign of the first derivative. This negative pressure dependence is due to the shift of the catalyst selectivity towards C_{2+} products.

The following reaction conditions were observed to yield best results as compared to the experimental data:

(a) Hydrogen and CO occupy different adsorption sites.
(b) The rate-limiting reaction step is α-hydrogenation.
(c) Hydrogen diffusion is fast.
(d) The probability for the β-dehydrogenation is lower than that of the α-hydrogenation.
(e) The chain growth is slow compared to the majority of the surface reactions.
(f) The potential barrier for the CO dissociation is low, i.e. the probability is of the same order as that for a typical surface reaction (much more probable than α-hydrogenation).
(g) The water removal reaction is relatively fast.

The simulation model has similar trends for the hydrocarbon formation as the experiment (see Fig. 10), which demonstrates that our approach offers an effective alternative to the traditional reaction kinetics modeling based on the set of the differential equations. The approach presented here may thus turn out to be useful tool for the interpretation of the experimental data also for other catalytic reactions.

After extensive simulations throughout the available parameter space, we were able to reproduce the experimental trends in the CO partial pressure dependence of C_{1-4} hydrocarbons and obtained also a fair agreement in the case of hydrogen partial pressure dependence and in the alkane/alkene ratio. The most serious drawbacks of the present model are the far too low selectivity towards methane, and some systematic deviations of the rate of C_{2+} formation at lowest CO pressures.

Finally, the model was employed to address the ensemble effects and structure sensitivity of the CO hydrogenation reaction. These simulations serve as a demonstration of the use of the reaction model to general aspects of the synthesis, and are not directly related to our comparison to the experiments. These results show that ensemble effects of CO dissociation are here of no importance in explaining the trends of the hydrocarbon formation. In the extreme case, when CO dissociation involves too many adsorption sites, catalyst poisoning is observed. Also simulation results on the hexagonal and square surfaces were similar, showing little structure sensitivity in pleasing agreement with the experimental evidence.

ACKNOWLEDGMENTS

This work has been made possible by generous computer resources from the Center of Scientific Computing, Espoo, Finland. J.-P.H. gratefully acknowledges financial support from Neste Foundation, Emil Aaltonen Foundation, and the Foundation of Financial Aid of Helsinki University of Technology.

[1] J. M. Smith, *Chemical Engineering Kinetics* (McGraw-Hill, New York, 1981).
[2] R. M. Ziff, E. Gulari, and Y. Barshad, Phys. Rev. Lett. **56**, 2553 (1986).
[3] H-P. Kaukonen and R. M. Nieminen, J. Chem. Phys. **91**, 4380 (1989).
[4] R. Imbihl, A. E. Reynolds, and D. Kaletta, Phys. Rev. Lett. **67**, 275 (1991).
[5] J-P. Hovi, J. Vaari, H-P. Kaukonen, and R. M. Nieminen, Comput. Math. Sci. **1**, 33 (1992).
[6] K. Yaldram and M. A. Khan, J. Catal. **131**, 369 (1991); B. J. Brosilow and R. M. Ziff, *ibid*. **136**, 275 (1992); K. Yaldram and M. A. Khan, *ibid*. **136**, 279 (1992).
[7] J. Lahtinen, T. Anraku, and G. A. Somorjai, J. Catal. **142**, 206 (1993).
[8] G. A. Mills and F. W. Steffgren, Catal. Rev. **8**, 159 (1973).
[9] P. K. Agraval, J. R. Katzer, and W. H. Manoque, Ind. Eng. Chem. **21**, 385 (1982).
[10] J. C. Geerlings, M. C. Zonneyville, and C. P. M. de Groot, Surf. Sci. **241**, 315 (1991).
[11] J-P. Hovi, J. Lahtinen, J. Vaari, and R. M. Nieminen, Surf. Sci. **311**, 331 (1994).
[12] J. Lahtinen, J-P. Hovi, and R. M. Nieminen, Catal. Lett. (in press).
[13] H. P. Bonzel and H. J. Kebbs, Surf. Sci. **117**, 639 (1982).
[14] J. Lahtinen, T. Anraku, and G. A. Somorjai, Catal. Lett. **25**, 241 (1994).
[15] H. Papp, Surf. Sci. **129**, 205 (1983).
[16] V. Ponec, Catal. Rev. **11**, 41 (1975).
[17] R. D. Kelley and D. W. Goodman, Surf. Sci. **123**, L743 (1982).
[18] M. Logan, A. Gellman, and G. A. Somorjai, J. Catal. **94**, 60 (1985).
[19] J. A. Rodriguez and D. W. Goodman, Surf. Sci. Rep. **14**, 1 (1991).
[20] J. C. Geerlings, M. C. Zonneyville, and C. P. M. de Groot, Surf. Sci. **241**, 302 (1991).